PERFORMANCE OF 3-D WOVEN COMPOSITES UNDER SHOCK LOADING

Arun Shukla[1], S Arjun Tekalur[1], Carl Rousseau[1], Alexander Bogdanovich[2], James Le Blanc[3]
shuklaa@egr.uri.edu
[1] University of Rhode Island, [2] 3TEX, Inc, [3] Naval Undersea Warfare Center

Keywords: *Shock loading, Blast, Textile composite, 3-D weaving, High speed photography, 3-D analysis, Dynamic analysis*

Abstract

The effects of highly transient shock loading on 3WEAVE™ composite material plates and sandwiches made with 3WEAVE™ composite skins and TRYMER™ 200L polyisocyanurate foam core have been studied experimentally. Some of the experimental work was supported by 3-D dynamic analysis. The experimental program is focused on recording dynamic transient response by high-speed camera and post-mortem evaluation of imparted damage. Some experiments also utilized strain gages and included residual deflection measurements. The obtained experimental results reveal important features of the transient deformation, damage initiation and progression and final failure modes in composite plates and sandwich panels with unstitched and stitched foam cores. The theoretical work demonstrates 3-D dynamic analysis of displacement, stress and strain fields in composite plates exposed to blast loading, using 3-D MOSAIC analysis tools. A comparison of experimental and theoretical strain histories at selected location of composite plate exposed to blast loading shows their excellent agreement.

1 Introduction

The present study is focused on evaluation of the blast performance of 3-D woven composite laminates and sandwiches made from 3WEAVE™ composite skins manufactured by 3TEX, and TRYMER™ 200L polyisocyanurate foam core produced by Dow Chemical. Also, the new sandwich-type material, named TRANSONITE, which is manufactured by Martin Marietta Composites, is used in this study. It is made from 3WEAVE™ preforms used for the skins and TRYMER™ 200L foam used for the core; they are stitched together by E-glass roving prior to the resin infusion. The stitch spacing can be varied. After the resin is infused into the skin preforms and through-thickness stitches and composite is consolidated, a thick composite sandwich is produced. It is characteristic with enhanced through-thickness compressive stiffness, strength and fracture toughness, as well as increased interface strength between the skins and core. This type of material has great potential for the applications where it is required to combine light weight, good structural load-bearing ability, efficient blast mitigation capability, high impact resistance, damage tolerance and general survivability.

The performance of aforementioned 3-D reinforced composite and sandwich materials exposed to highly transient blast loading is studied here both experimentally and theoretically. In the recent publication of this group of authors [1], a comprehensive experimental study was presented for several typical 3WEAVE™ reinforced composites exposed to different levels of blast pressure formed in the new shock tube built at the University of Rhode Island. The present paper continues that study and reports first experimental results of the blast testing and post-mortem damage evaluation of TRANSONITE composite sandwich panels having 3WEAVE™ skins and through-thickness stitched cores. The experimental work is supported by the new theoretical study based on the analysis approach described in [2-5] that helps to understand complex deformation, damage and failure phenomena observed in the conducted blast loading experiments.

In recent times, several researchers have pursued studies on characterization of different core materials and sandwich composite structures under dynamic loading, see [6-8] for example. The overall dynamic response of the sandwich is dependent, among several other factors, on the construction of the skin, compressive modulus and failure strength of the core, and the interface strength between the

skin and core. Particularly, Z-directional pins have been utilized in [7] to modify the sandwich material; its high strain rate impact response was then studied. Authors of [8] studied failure modes of carbon fiber based sandwich beams reinforced with Z-directional pins under three-point bending. Yet, to the best of these authors' knowledge, there are no reported experimental or theoretical results on the deformation and failure behavior of sandwich composites incorporating 3-D woven composites skins and transversely reinforced foam core. Particularly, this applies to any kind of dynamic loading. As the results of this paper show, the through-thickness reinforcement of the foam core significantly increases its compressive stiffness and strength, radically changes the whole dynamics of transient deformation and, as the result, substantially reduces overall damage imparted to the sandwich composite.

2 Materials

2.1 Composite Panels and Sandwich Skins

The skin materials utilized in this study were made by VARTM method from 3WEAVE™ S-2 and E-glass glass roving preforms with Dow Derakane 8084 epoxy-vinyl ester resin. Four different composite materials of this kind, made from S-2 glass fiber, were investigated under blast loading in [1]. That paper provides complete description of all four preform constructions. Here we will include some of the previous test data for only one of those composites, which was made with two layers of preform having 3.15 kg/m^2 (93 oz/yd^2) areal density, and only for the purpose of experimental validation of the analysis approach.

The fabricated preform and composite made thereof are shown in Fig. 1. Geometrical models of the preform and composite Unit Cell are shown in Fig. 2.

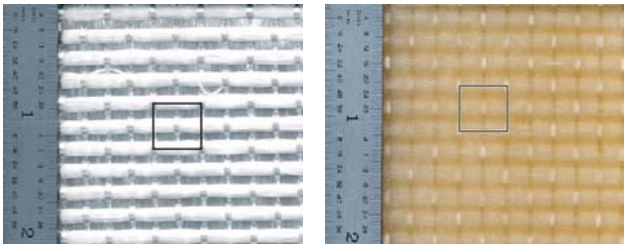

Fig. 1. 3WEAVE™ S-2 glass preform (left) and its Derakane 8084 epoxy/vinyl ester composite (right) used in this study. The Unit Cell shown in frame

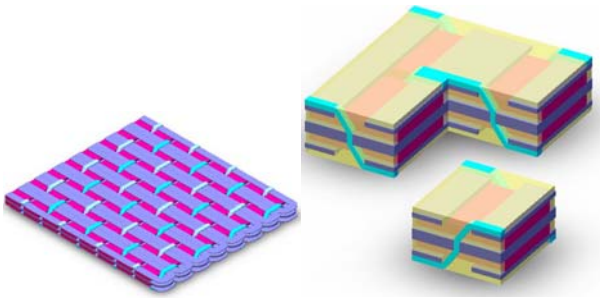

Fig. 2. Geometric model of 3.15 kg/m^2 areal density 3WEAVE™ fabric (left) and its composite Unit Cell (right)

The preform has 2 warp fiber layers and 3 fill (a.k.a. weft) fiber layers. S-2 glass 250 yield/lb roving was used for both warp layers with 10 ends/inch insertion spacing. S-2 glass 750 yield/lb roving was used for the top and bottom fill layers, while 250 yield/lb roving was used for the middle fill layer (all fill yarns inserted with 5.5 picks/inch spacing). S-2 glass 1250 yield/lb roving was used in Z-direction (5 ends/inch insertion). The described fabric construction is slightly unbalanced with respect to the fiber volume content in the warp direction (50.8%) and fill direction (45.6%). The volume fraction of Z-fiber is 3.6%. The total fiber volume fraction in the composite was determined as 49%. The described 3WEAVE™ S-2 glass fiber preform was used in the 2-layer composite test specimen [1] and also in one type of composite skins used in the sandwich specimens studied here.

2.2 Core Material

The core material used in the sandwich was made of Dow Chemical TRYMER™ 200L polyisocyanurate foam, which is a cellular polymer. This foam is specified to be ideal for applications in which a lightweight, low-density core is needed; the foam is less brittle than conventional polyisocyanurate foams. This foam is compatible with most thermoset resins, including vinyl esters and epoxies. From the manufacturer's data, the density of the foam is 32 kg/m^3. Its tensile, compressive and shear moduli parallel to rise are 8.27, 5.17 and 1.79 MPa respectively. Its tensile (3-D average), compressive (parallel to rise) and shear (average of parallel to rise and extruded directions) strengths are 0.207, 0.207 and 0.159 MPa respectively.

2.3 Sandwich Constructions

The tested sandwich materials, produced by Martin Marietta Composites, were constructed out of 3WEAVE™ fabrics in the skins and unstitched or stitched TRYMER™ 200L foam core. Two different types of glass fibers, S-2 glass and E-glass were used in the skins. In all samples the first two layers of the front skin (exposed to blast pressure) were made of the standard 0.81 kg/m^2 (24 oz/yd^2) areal density 2-D E-glass plain weave. Those were followed by three layers of either 3.15 kg/m^2 S-2 glass 3WEAVE™ or three layers of 3.25 kg/m^2 (96 oz/yd^2) E-glass 3WEAVE™. The back skins contained (counting from the back surface of the foam) two layers of either 3.15 kg/m^2 S-2 glass 3WEAVE™ or 3.25 kg/m^2 E-glass 3WEAVE™ followed by two layers of the same E-glass plain weave.

Each of the aforementioned skin constructions, containing either E-glass or S-2 glass 3WEAVE™ preforms, was used with the foam to make a sandwich. The first sandwich type was not stitched through the thickness. The second type had 4 insertions/in^2 stitch spacing, and the third type had 8 insertions/in^2 stitch spacing. In all cases 103 yield/lb E-glass roving was used for stitching. Table 1 summarizes construction characteristics of six different sandwich panels that were used in this study. Thickness of the core was ~50 mm, thickness of the front skin in the range of 8-9 mm and thickness of the back skin in the range of 6-7 mm.

Table 1. Construction of the sandwich composite specimens used in this study

Specimen Name	Front Skin	Back Skin
Sandwich 1 (R = 0)	2 layers of A + 3 layers of B	2 layers of B + 2 layers of A
Sandwich 2 (R = 4)	2 layers of A + 3 layers of B	2 layers of B + 2 layers of A
Sandwich 3 (R = 8)	2 layers of A + 3 layers of B	2 layers of B + 2 layers of A
Sandwich 4 (R = 0)	2 layers of A + 3 layers of C	2 layers of C + 2 layers of A
Sandwich 5 (R = 4)	2 layers of A + 3 layers of C	2 layers of C + 2 layers of A
Sandwich 6 (R = 8)	2 layers of A + 3 layers of C	2 layers of C + 2 layers of A

Note:
A - 0.81 kg/m^2 E-glass plain weave
B - 3.25 kg/m^2 E-glass 3WEAVE™
C - 3.15 kg/m^2 S-glass 3WEAVE™
R - Number of stitches per in^2

3 Experimental Method

3.1 Loading Apparatus – Shock Tube

Fig. 3 depicts the shock tube apparatus used in this study to obtain the controlled blast loading. In principle, the shock tube consists of a long rigid cylinder, divided into a high-pressure driver section and a low pressure driven section, which are separated by a diaphragm. By pressurizing the high-pressure section, a pressure difference across the diaphragm is created. When this difference reaches a critical value, it ruptures. This rapid release of gas creates a shock wave, which travels down the tube to impart dynamic loading on the specimen. The specimen is held in fixture that ensures proper specified boundary conditions.

Fig. 3. The shock tube facility

The shock tube utilized in the present study has an overall length of 8 m, consisting of a driver, driven and muzzle sections. The diameter of the driver and driven section is 0.15 m. The final muzzle diameter is 0.07 m. A pressure sensor (PCBA23) mounted at the end of the muzzle section measures the impact shock pressure and the reflected pressure during the experiment. Typical pressure profile obtained at the sensor location is shown in Fig. 4. The velocity of the shock wave was measured using trigger circuits and was determined as ~1100 m/s (Mach 3.3) in these experiments.

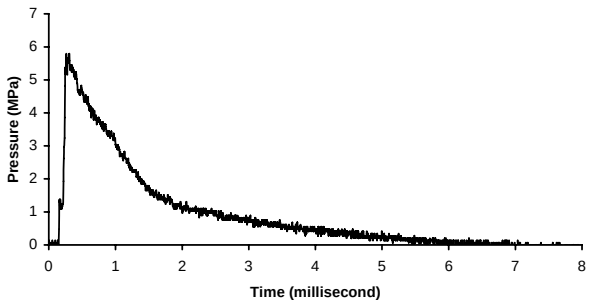

Fig. 4. Typical incident blast pressure profile

3.1 Boundary Conditions

In the previous experiments involving the all-S-2 glass composite materials [1], the tested square

panels were of in-plane size 0.35 m x 0.35 m with an approximate thickness of 6.35 mm. The specimens having dimensions 0.23 m x 0.23 m of unsupported test section were held under fully clamped (fixed) boundary conditions, as shown in Fig. 5. The blast was applied over a circular area 76 mm in diameter.

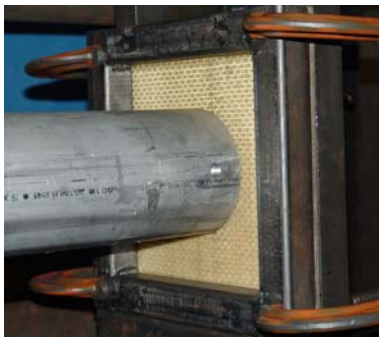

Fig. 5. 3WEAVE™ composite plate clamped in the fixture with the muzzle of shock tube shown

In the experiments involving sandwich materials, the rectangular specimens were under simply supported boundary conditions, as shown in Fig. 6. The specimen size was 0.30 m x 0.102 m. The span between supports was 0.152 m. As in the previous case, the blast load covered circular central region of the specimen 76 mm in diameter.

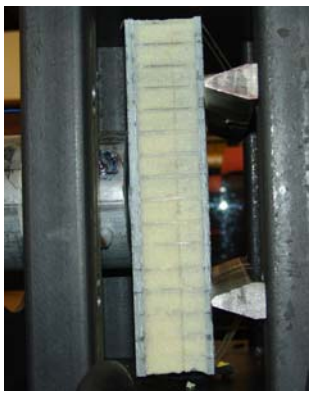

Fig. 6. Simply supported sandwich composite plate with the muzzle of shock tube shown

4 Experimental Results

4.1 3WEAVE™ S-2 Glass Composite Plates Under Blast Loading

With reference to [1], we summarize here that the appearing visual damage of the composite test panels was taken as an initial indicator of the amount of damage imparted during the blast event. Typically, damage observed on the surface of the specimen consisted of surface discolorations, fiber breakage and cracking; the amount of each type damage is dependent upon the blast pressure level.

Several panels were cross sectioned for internal damage inspection with a stereoscopic microscope. The internal damage mechanism consisted mainly of internal fibre breakage. As illustrated by specific results in [1], the amount of visual damage is found to increase with shock level. In the areas corresponding to the greatest amount of surface fiber breakage, internal delamination cracks with breakage of the through-thickness (Z-directional) fiber were found. This observation leads to the indication that the severity of the transverse (through-thickness) tensile stress wave was capable of breaking 1250 yield/lb S-2 glass roving and creating delamination cracks.

Other experimental studies in [1] associated with blast loading of four different S-2 glass 3WEAVE™ composite panels included residual compressive strength characterization and permanent deformation mapping. The experimental study also included some transient strain measurements using strain gages mounted at selected locations of the back surface of the plate. An example of such strain history will be shown and used for comparison with predictive analysis results in Section 5 of this paper.

4.2 Composite Sandwiches Under Blast Loading

4.2.1 Real time observations

The dynamic transient behavior of sandwich panels was recorded using a high resolution digital camera and thoroughly analyzed. The results corresponding to different time instants are shown in Fig. 7 for Sandwich 1 (see Table 1), in Fig. 8 for Sandwich 2 and in Fig. 9 for Sandwich 3.

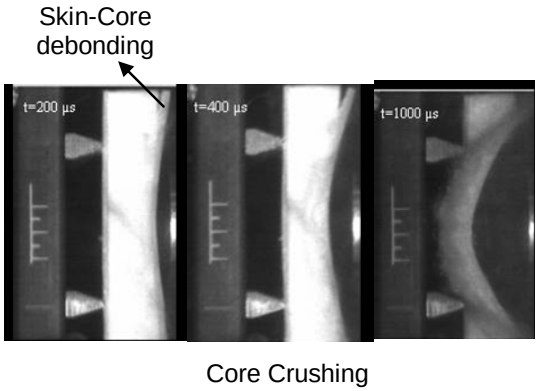

Fig. 7. Real-time observation of Sandwich 1 using high-speed camera

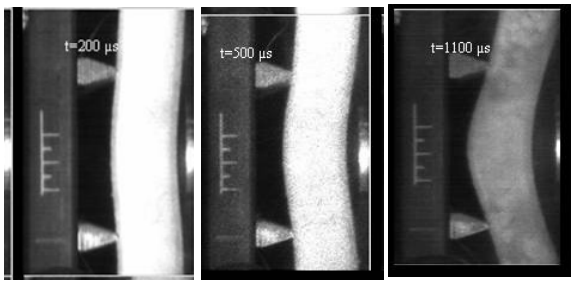

Fig. 8. Real-time observation of Sandwich 2 using high-speed camera

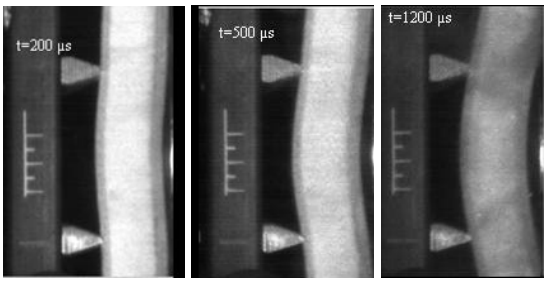

Fig. 9. Real-time observation of Sandwich 3 using high-speed camera

These figures well illustrate the observed specifics of transient deformation and damage development processes in each case. It is obvious that through-thickness stitching of the core makes dramatic effect on these processes. In case of Sandwich 1, where the core is unstitched, relatively soft foam, the back skin remains nearly undeformed even at $t = 500\mu\text{sec}$ when the front skin has been already deeply indented into severely damaged core. In fact, in this case the front and back skins deform almost independently; the high blast pressure applied to the front skin is substantially weakened when it arrives at the back skin. The measurements showed that at $t = 500\mu\text{sec}$ central deflection is about 5.5 times higher for the front skin than for the back one. Also note in Fig. 7 that initial separation of one of the edges of the front skin from the core is observed at $t = 200\mu\text{sec}$; this indicates their relatively weak adhesion.

Fig. 8 shows a very different deformation pattern. In this case the blast pressure is much better transferred from the front to the back of the sandwich, and we see kind of 'in-sync' local bending of both skins and core layer between them. Of course, the core is gradually damaged as such bending progresses. As measurements showed, the difference between central deflection of the front and back skins is just a few percent. Also, no separation between the front skin and the core is seen in these high-speed camera frames.

Fig. 9 shows the sandwich deformation pattern which is very similar to the one seen in Fig. 8. The only significant difference is in the deflection values which are at $t = 500\mu\text{sec}$ about 30% smaller at the center of the plate in case of Sandwich 3. Obviously, additional core stiffening reduces overall deflection of the sandwich.

The major failure mechanism evident in Fig. 7 is progressive damage of the core which starts with some dispersed damage near the front skin and simultaneous formation of a large inclined crack in the central region of the core. These two damage zones gradually extend and coalesce at approximately $t = 400\mu\text{sec}$ which is followed by the formation of a much larger damage zone at $t = 500\mu\text{sec}$ and rapid crush of the core after that. Probably, around the same time instant the front skin suffers significant failure, although it is difficult to see it in Fig. 7. Likely, the back skin fails soon after that, and the whole sandwich is crushed. The conclusion is that Sandwich 1 can not withstand the applied blast pressure which has peak value ~ 5.24 MPa reached at $\sim t = 60\mu\text{sec}$ (the pressure history is of the same type as shown in Fig. 4).

Contrary to the case of Sandwich 1, the real time deformation sequences seen in Fig. 8 for Sandwich 2 and in Fig. 9 for Sandwich 3 indicate that the reinforced core damage does not include any visible macro-crack initiation and propagation, although one can see certain micro-damage accumulation and propagation from frame to frame. It is hard to reveal the skin damage and failure peculiarities from Figs. 8 and 9, so additional post-mortem evaluation of the tested sandwich panels has been performed.

4.2.2 Micrographic post-mortem observations

Some results of post-mortem evaluation are shown in Fig. 10. In Sandwich 1 sample, the core did disintegrate completely and was lost beyond retrieval. The front skin (which is top in Fig. 10a shows severely fractured fibers in the central region (where blast pressure was applied); it also delaminated into two layers there. The back skin, as is seen in Fig. 10a, did completely delaminate along the interface between two 3-D woven composite layers and separated into two pieces having thicknesses 2.92 mm and 3.86 mm. Contrary to that, Fig. 10b shows only localized delaminations in the skins along with some foam damage in the core. The

damage in this case is confined to the mid-section on the front skin and minimal visual damage of the back skin. The observed permanent deformation of this sandwich sample is relatively small. Separation of the core chunks from the stitch yarns was observed in this sample. Buckling of the stitches themselves was observed under visual examination. The location of this buckling was identified by bright white shear-like spots on the side view of the panels; interestingly, it was detected closer to either of the skins rather than in the mid-region of the core.

Further on, Fig. 10c shows very minimal damage in the skins and core and practically no overall permanent deformation of the sandwich panel. Except for a minor visual damage, both front and back faces showed no signs of fiber breakage or other failure types. Cracks parallel to the stitches were found in the core. Overall, it can be concluded that this sandwich fully survived the blast loading.

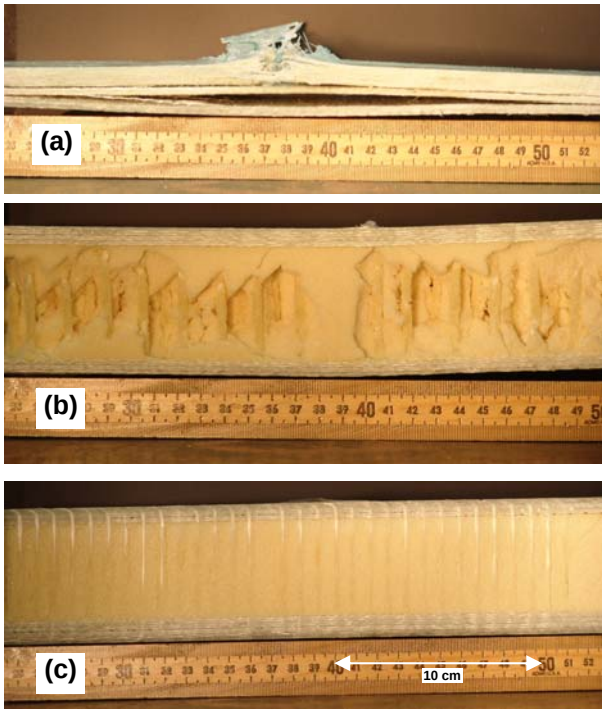

Fig. 10. Side views of Sandwich 1 (a), Sandwich 2 (b) and Sandwich 3 (c) panels after blast testing

Similar results have been observed for the other three samples, namely Sandwich 4, Sandwich 5 and Sandwich 6, where skins were made with S-2 glass roving (see Table 1). The damage pattern generally followed the same trend as discussed above for E-glass skin sandwiches, vis-à-vis, as the core reinforcement increased, the damage initiation was delayed and its extent decreased. However, Sandwich 4 sustained the same level of blast loading better than its counterpart Sandwich 1. This result was deduced from the macroscopically observed extent of core damage and delaminations. It was also concluded from the post-mortem observations of S-2 glass sandwiches that core stitches showed more pronounced buckling and qualitatively higher core separation than in the E-glass sandwiches. It was also concluded from comparison of Sandwich 6 and Sandwich 3 that for the former one the blast pressure transfer from the front face to the back face was quantitatively higher and the core was better involved in the transient deformation process. A more detailed discussion and illustration of blast testing results for the S-2 glass and E-glass sandwich panels will be presented elsewhere.

5 Computational Modeling

3TEX's analysis approach and in-house computer code 3-D MOSAIC, based on the theory and algorithms described in [2,3], has been earlier applied to several specific blast modeling problems, see [4,5]. Here we illustrate application of this computational tool to the problem of 3-D transient deformation of a 2-layer 3WEAVE™ 3.15 kg/m^2 areal density S-2 glass reinforced composite plate experimentally studied in [1] (see summary of that study in Sections 3 and 4.2 above). Next sections describe the problem formulation, provide illustrative numerical results with convergence study, and show some comparisons with experimental data.

5.1 Problem Formulation

Following experimental setup described in Section 3, the boundary value problem was stated as follows. The analyzed ¼ of a square homogeneous composite plate is shown in Fig. 11. Length of its out-of-clamp area is $a = 0.2286m$ and its thickness is $c = 6.35mm$. Boundary conditions at the clamped side edges $x = 0$ and $y = 0$ are taken as

$$u_x = 0,\ u_z = 0 \ \text{at}\ x = 0 \ \text{for all}\ z \qquad (1)$$

$$u_y = 0,\ u_z = 0 \ \text{at}\ y = 0 \ \text{for all}\ z \qquad (2)$$

The symmetry boundary conditions were set along vertical mid-sections of the plate as follows

$$u_x = 0 \ \text{at}\ x = a \ \text{for all}\ z \qquad (3)$$

$$u_y = 0 \ \text{at}\ y = a \ \text{for all}\ z \qquad (4)$$

The coordinate system is shown in Fig. 11.

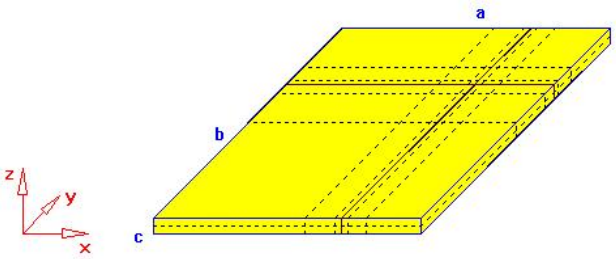

Fig. 11. Computational model of ¼ of the plate analyzed.

Central part of the front (top in Fig. 11) surface of the plate is loaded by either uniformly distributed or half-sine wave distributed dynamic pressure within square region $a_0 \times a_0$, hence, the loading region is defined as

$$a - a_0 \le x \le a, \quad a - a_0 \le y \le a \quad \text{at} \quad z = c \tag{5}$$

The value $a_0 = 0.03376m$ was determined by equalizing area of the square region $a_0 \times a_0$ with the area of ¼ circle having radius $r = 0.0381m$, in order to get total loading area as in the actual experiment.

The time variation of incident blast pressure is taken in the following form:

$$P(t) = P_0 \cdot t^n \cdot e^{-B \cdot t} \tag{6}$$

where t is in μsec and P_0 is in MPa. Numerical values of parameters in equation (6) are

$$P_0 = 1.717MPa, \; n = 0.09, \; B = 0.00429\mu\sec^{-1} \tag{7}$$

These values were obtained from the smooth approximation by function (6) of experimental 'reflected' pressure (of the type shown in Fig. 4) recorded in experiments, see details in [1]. The peak value of $P(t)$, reached at $t_0 = 210\mu$sec, is $P(t_0) = 2.54MPa$.

In the case of half-sine wave surface load distribution along coordinates x and y, the P_0 value in (6) has to be increased by factor $(\pi/2)^2$ in order to keep the equivalency with the total surface load acting on the plate in the case of uniform surface distribution. So, in this case we shall use $P_0 = 6.27MPa$.

The following material properties have been used in this analysis for 3-D woven composite material under consideration:

$$E_x = 26.5GPa, \; E_y = 27.0GPa, \; E_z = 12.5GPa \tag{8}$$

$$G_{xy} = G_{xz} = 3.5GPa, \; G_{yz} = 3.3GPa \tag{9}$$

$$\nu_{xy} = 0.11, \; \nu_{xz} = 0.34, \; \nu_{yz} = 0.33 \tag{10}$$

$$\rho = 1850kg/m^3 \tag{11}$$

5.2 Numerical Examples and Convergence Study

Computational mesh used in the analysis is shown in Fig. 11. One of the advantages of 3-D MOSAIC approach is that in order to study convergence of numerical results, one may keep constant discretization mesh and vary the degree of Bernstein approximation polynomials used as the basis functions. More details on convergence analysis methodology can be found in [5].

Figs. 12 and 13 illustrate one example of such convergence study – the computed history of transverse displacement $u_z(t, x = a, y = a, z = c)$ and in-plane strain $\varepsilon_x(t, x = a, y = a, z = c)$ at the center of the plate on top surface are plotted for half-sine blast load distribution applied within square region (5). Numerical solutions with polynomial degrees 1, 2 and 3 were mutually compared. It is seen in the figures that for both the displacement and strain, the curve corresponding to degree 1 is much different from the ones corresponding to degrees 2 and 3, while the latter two curves are very close. Other studies have shown that numerical results for transverse strains and stresses converge slower than numerical results for displacements and in-plane strains and stresses. Nevertheless, by selecting appropriate discretization mesh and polynomial degree, converged results can be obtained for all 3-D stress/strain components.

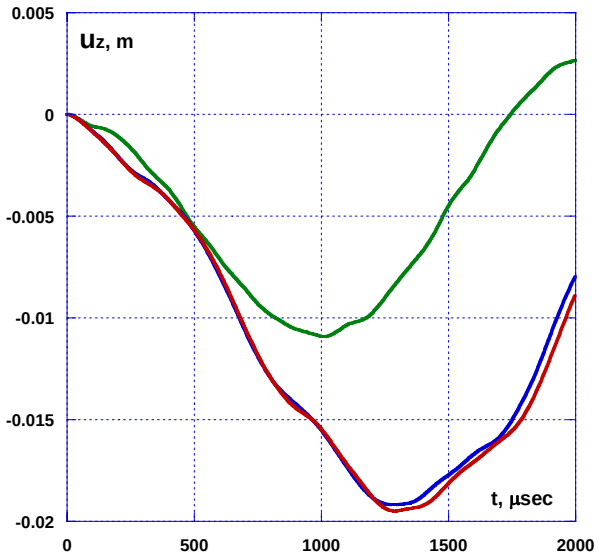

Fig. 12. Results for central deflection computed with polynomial degrees 1 (green), 2 (blue) and 3 (red)

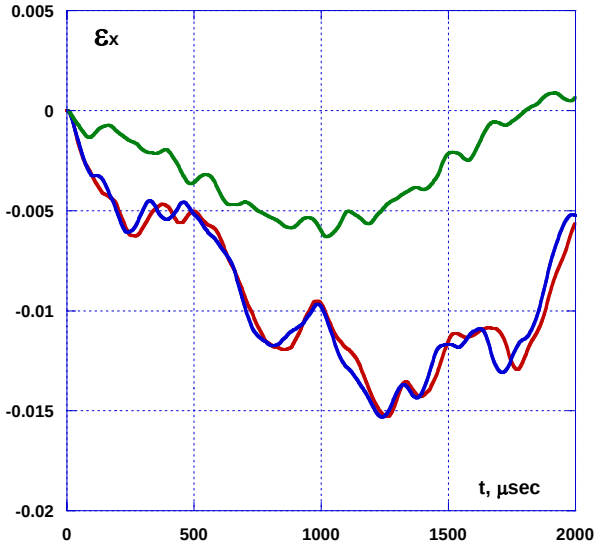

Fig. 13. Results for strain ε_x computed with the use of polynomial degrees 1 (green), 2 (blue) and 3 (red)

Further, Fig. 14 shows comparison of the computed transverse displacement histories for the cases of half-sine and uniform distributions of blast pressure applied to region (5). Polynomial degree 3 was used in both analysis cases. It is seen in the figure that the curves for deflection at the center of the plate slightly differ, and this is not a surprise because blast pressure at the center is ~2.5 times higher in the case of half-sine distribution. However, another two curves, corresponding to the point outside the loading area, are practically identical.

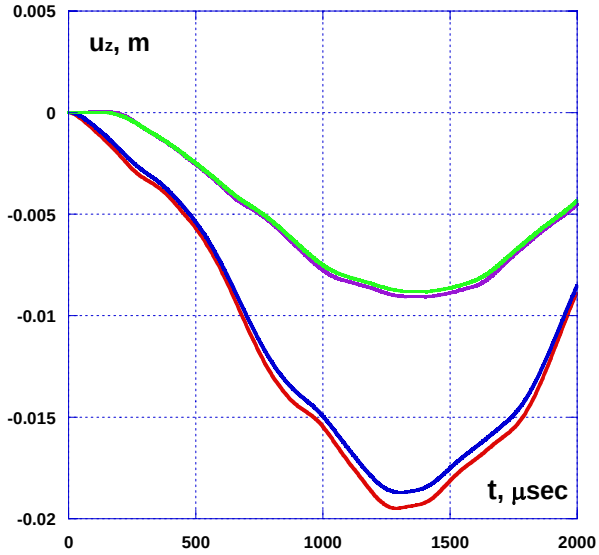

Figure 14. Comparison of plate deflection computed with uniform (blue and green) and half-sine (red and purple) blast pressure distributions at the center of the plate at its front surface (red, blue) and at $x = a$, $y = a/3$ on back surface (purple, green)

5.3 Comparison with Experimental Data

Next we compare some of the analysis results with experimental data. Fig. 15 shows experimental blast pressure history at the center of the plate, its approximation by smooth function (6), which was used as input data in the analysis, and computed time variation of the stress component $u_z(t, x = a, y = a, z = c)$, which would exactly match (6) if 'exact' numerical solution had been obtained. However, as any numerical solution, this solution is not exact, and though the general similarity between the blue and green curves in Fig. 15 is obvious, there are also certain differences between them. Particularly, the computed stress history is quite irregular and has small fluctuations, while those are absent in the blue curve. However, from the viewpoint of such irregularities and fluctuations, the green curve has much more similarity with the red one (experimental). It should also be noted that it is most challenging to accurately predict transverse normal stress component in 3-D analysis of plates in general. Hence, the obtained very good agreement between the computed transverse normal stress and respective boundary condition on one side, and between computed stress and experimental blast pressure on the other, let us expect that this numerical solution predicts all other displacement, strain and stress components with no less accuracy.

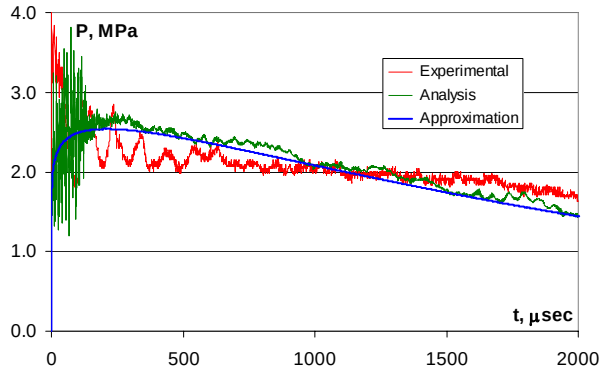

Fig. 15. Experimental blast pressure history, its approximation by smooth function (6), and computed stress history at the center of front surface

One example of comparison between theoretically predicted and experimentally recorded strain is shown in Fig. 16. Keeping in mind the difficulties of reliably measuring transient strains under shock wave on one side, and complexity of 3-D transient analysis performed, the agreement between theoretical and experimental results is very impressive. The characteristic negative strain in the first phase of deformation (before 500 μsec) is almost identical in the experimental and theoretical results (especially those obtained with half-sine load distribution). The second, positive strain phase (between 500 and 2000 μsec) seen in experimental curve is also present in the theoretical curves, and the experimental peak strain values are very close to the theoretical ones.

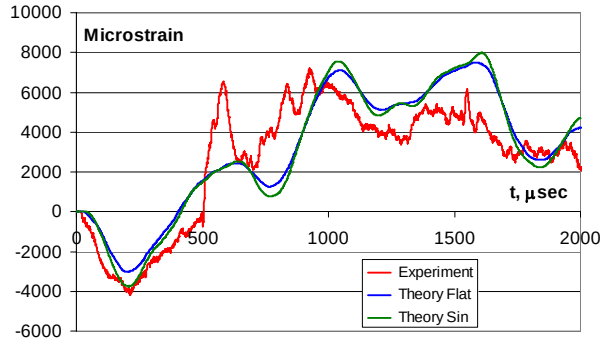

Fig. 16. Experimental strain (red) and theoretical strains predicted by analyses with uniform (blue) and half-sine (green) blast pressure distributions

Some differences between theoretical and experimental curves observed in Fig. 16 may be caused, as we hypothesize, by not fully adequate simulation of the actual plate clamping conditions by the imposed boundary conditions (1) and (2). Indeed, in the actual experiment set up, about 38 mm (1.5 inch) wide area of the plate on all four sides is placed within the clamp, so the in-plane stress wave coming from the blast loading zone is allowed to further propagate along the plate within clamp area and reflect there. At the same time, boundary conditions $u_x = 0$ in (1) and $u_y = 0$ in (2) mean that the plate is placed within a "rigid box" where the clamp frame begins. Future work will clarify this issue.

The first of its kind comparison between theoretical and experimental results for the strain generated by blast loading and its success demonstrated in Fig. 16, is a culmination of this work. This initial effort is currently extended to the case of transient deformation and failure analysis of composite sandwich panels which experimental study has been presented in Sections 3-4 of this work.

6 Conclusions

Experimental methodology of material testing in shock wave tube, developed by this group of authors and previously used for blast testing of 3WEAVE™ composite plates, is applied in this paper to six different TRANSONITE sandwich constructions. Those differ in the skin materials (E-glass vs. S-2 glass fibers in 3-D woven skin preforms), and also in the core material, which is based on TRYMER™ 200L polyisocyanurate foam. Two sandwiches contain pristine foam as the core, while the other four have skin preforms and the core integrally stitched together with different stitch spacing.

The results of the blast tests include real time images of the deflection and progressive damage of the skins and core. Those are supplemented by visual post-mortem examination, including residual deformation and damage evaluation which provided additional insight into the effect of 3-D skin and core construction and properties on the performance of sandwich composites under blast loading. Generally, the sandwich composites with through-thickness stitch reinforcement in the core are characteristic with much lower dynamic deformation, delayed damage initiation and higher dynamic damage tolerance with minimal visual residual damage.

The first of its kind comparison between theoretically predicted dynamic transverse normal stress vs. applied blast pressure and surface strain vs. its experimental reading by strain gage during blast loading of 3WEAVE™ composite plate, showed their excellent agreement. This demonstrates the

ability of 3-D MOSAIC analysis tool to adequately model complex blast loading experiments and accurately predict transient strains and stresses during milliseconds long blast loading. Computational modeling of composite sandwich blast tests reported here is underway.

7 Acknowledgements

The first two authors acknowledge the financial support from the Office of Naval Research under grant no. N000140410268. The financial support from the URI Transportation Center under grant numbers 500-2304-0000-0000057 and 500-2304-0000-0000507 is also acknowledged.

The authors are thankful to Martin Marietta Composites company for supplying sandwich materials used in this study.

8 References

[1] LeBlanc, J., Shukla, A., Rousseau, C. and Bogdanovich, A. “Shock loading of three-dimensional woven composite materials”. *Composite Structures*, Vol. 79, No. 3, pp 344-355, 2007.

[2] Bogdanovich, A.E. "Three-Dimensional Variational Theory of Laminated Composite Plates and Its Implementation with Bernstein Basis Functions". *Computer Methods in Applied Mechanics and Engineering*, Vol. 185, No. 2-4, pp. 279-304, 2000.

[3] Bogdanovich, A.E. and Yushanov, S.P. "Three-Dimensional Variational Impact Contact Analysis of Composite Bars and Plates". *Composites Part A: Applied Science and Manufacturing*, Vol. 31A, No. 8, pp. 795-814, 2000.

[4] Bogdanovich, A.E. and Yushanov, S.P. "3-D Blast Performance Analysis of Concrete Walls with Layered Composite Protection/Retrofit". *Proceedings – 14th Technical Conference of The American Society for Composites*, Dayton, OH, pp. 151-160, 1999.

[5] Bogdanovich, A.E. and Mungalov, D.D. “Three-Dimensional Blast Response Simulation of Layered Composite Armor Panels”. *Proceedings - 3rd International Conference on Structural Stability and Dynamics (ICSSD)*, Kissimmee, FL, 2005.

[6] Mahfuz, H., Thomas, T., Rangari, V. and Jeelani, S. “On the Dynamic Response of Sandwich Composites and Their Core Materials”. *Composites Science and Technology*, Vol. 66, No. 14, pp. 2465-2472, 2006.

[7] Vaidya, U.K., Nelson, S., Sinn, B. and Mathew, B. "Processing and High Strain Rate Impact Response of Multi-Functional Sandwich composites". *Composite Structures*, Vol. 52, pp. 429-440, 2001.

[8] Rice, M.C., Fleischer, C.A. and Zupan, M. “Study on the Collapse of Pin-Reinforced Foam Sandwich Panel Cores“. *Experimental Mechanics*, Vol. 46, No. 2, pp. 197-204, 2006.